Computers & Geosciences 36 (2010) 997–1004

Contents lists available at ScienceDirect

Computers & Geosciences

journal homepage: www.elsevier.com/locate/cageo

A multi-species reactive transport model to estimate biogeochemical rates based on single-well push–pull test data ☆

Mantha S. Phanikumar [a,*], Jennifer T. McGuire [b,1]

[a] Department of Civil & Environmental Engineering, Michigan State University, East Lansing, MI 48824, USA
[b] Department of Geology, University of St. Thomas, St. Paul, MN 55105, USA

ARTICLE INFO

Article history:
Received 29 September 2006
Received in revised form
26 March 2010
Accepted 1 April 2010

Keywords:
Push–pull test
Pump test
Inverse modeling
Microbial processes
Dispersion
Reaction
Sorption
In situ rate estimation
PPTEST
Mobile–immobile

ABSTRACT

Push–pull tests are a popular technique to investigate various aquifer properties and microbial reaction kinetics *in situ*. Most previous studies have interpreted push–pull test data using approximate analytical solutions to estimate (generally first-order) reaction rate coefficients. Though useful, these analytical solutions may not be able to describe important complexities in rate data. This paper reports the development of a multi-species, radial coordinate numerical model (PPTEST) that includes the effects of sorption, reaction lag time and arbitrary reaction order kinetics to estimate rates in the presence of mixing interfaces such as those created between injected "push" water and native aquifer water. The model has the ability to describe an arbitrary number of species and user-defined reaction rate expressions including Monod/Michelis–Menten kinetics. The FORTRAN code uses a finite-difference numerical model based on the advection-dispersion-reaction equation and was developed to describe the radial flow and transport during a push–pull test. The accuracy of the numerical solutions was assessed by comparing numerical results with analytical solutions and field data available in the literature. The model described the observed breakthrough data for tracers (chloride and iodide-131) and reactive components (sulfate and strontium-85) well and was found to be useful for testing hypotheses related to the complex set of processes operating near mixing interfaces.

1. Introduction

Push–pull tests are a commonly used technique for obtaining a wide range of *in situ* data including microbial transformations of hydrocarbons (Istok, 1997, 2001; Kleikemper et al., 2002; Pombo et al., 2002; Reinhard et al., 1997), radionuclides (Senko et al., 2002), electron acceptors (Harris et al., 2005; McGuire et al., 2002; Schroth et al., 1998), nutrients (Luthy et al., 2000), groundwater flow velocities (Leap and Kaplan, 1988), solute retardation (Schroth et al., 2001a), sorption (Davis et al., 2002; Istok et al., 1999; Istok, 2001), cation exchange (Drever and McKee, 1980) and aquifer properties (Hall et al., 1991; Pickens and Grisak, 1981). Push–pull tests consist of a controlled rapid injection of a test solution into a single well followed by the slow recovery of the test solution from the same well (Istok, 1997). Though push–pull tests vary based on their intent, most push–pull tests contain three phases (Fig. 1): (1) extraction of groundwater from the push–pull well for preliminary geochemical characterization; (2) injection (push) of a test solution containing reactive solute(s) and a conservative solute as a tracer to account for advection and dispersion and (3) extraction (pull) of the test solution, sometimes after an incubation period, and measurement of solute concentrations over time.

Several studies have used push–pull tests to describe *in situ* microbial reaction kinetics. Studies by Haggerty et al. (1998) and Snodgrass and Kitanidis (1998) provide simplified methods of calculating first and zero-order *in situ* microbial reaction rate coefficients. These studies account for decreases in solute concentration as a result of dilution from diffusion and dispersion and require no knowledge of aquifer porosity, dispersivity, or hydraulic conductivity, nor the use of flow and transport models. Several studies have used these methods to interpret rate data from push–pull tests for various chemical species (Cunningham et al., 2001; Harris et al., 2005; Istok, 2001; Kleikemper et al., 2002; Luthy et al., 2000; McGuire et al., 2002; Schroth et al., 2001b; Ulrich et al., 2003). However, rate data obtained from push–pull tests do not always follow the idealized example described in Haggerty et al. (1998), (see Fig. 2a), creating difficulties with interpretation. Complexities often observed in rate data include the presence of a lag phase, complex reaction order and the presence of multiple rate constants as shown in Fig. 2b. A lag phase prior to reaction has been observed for a wide

☆ Code available from server at http://www.iamg.org/CGEditor/index.htm

* Corresponding author. Tel.: +1 517 432 0851; fax: +1 517 355 0250.
E-mail addresses: phani@msu.edu (M.S. Phanikumar), jtmcguire@stthomas.edu (J.T. McGuire).
[1] Tel.: +1 651 962 5254; fax: +1 651 962 5209

0098-3004/$ - see front matter © 2010 Elsevier Ltd. All rights reserved.
doi:10.1016/j.cageo.2010.04.001

range of microbial transformations (Addy, 2002; Istok, 2001; Kleikemper et al., 2002; Kneeshaw et al., 2007; Luthy et al., 2000; McGuire et al., 2002; Schroth et al., 2001b). Though the cause of the lag phase varies and is a topic of ongoing studies, a simple analytical solution cannot describe the presence of a lag phase leading to an incomplete description of kinetic controls. This becomes particularly important when applying rate estimates to other systems. Another commonly observed complexity is the apparent "scatter" within first-order rate coefficient data. Though a best-fit line is often constructed, this is less than ideal and valuable information on the processes controlling kinetics can be obscured. Closer examination of data published in the literature shows poor linear fits due to trends in data that are curved or appear to have changes in slope suggesting multiple/fractional-order rate constants or multiple first-order rate constants, respectively (e.g., McGuire et al., 2002; Fig. 3 in their paper, Schroth et al., 1998; Fig. 6b, Haggerty et al., 1998; Fig. 7c and d, and Schroth et al., 2001b; Fig. 4). These changes in slope likely represent important shifts in physical, chemical or microbial processes that need to be considered to understand kinetic controls at the system scale. Inclusion of these complexities in the analysis and description of rate data is necessary to be able to accurately apply these rates to other systems or predict how rates might change over time.

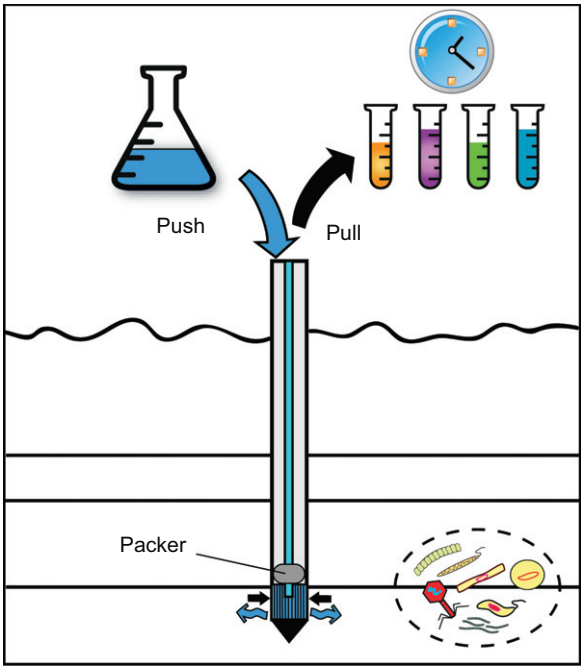

Fig. 1. Schematic diagram of a typical push–pull test.

Most of the previous research on modeling push–pull tests focused on finding approximate analytical solutions (Gelhar and Collins, 1971; Hsieh, 1986), using a semi-analytical solution (Haggerty et al., 1998) or using fairly general-purpose numerical codes to simulate the one-dimensional radial flow problem. Hoopes and Harleman (1967) presented a finite-difference scheme using a central weighting approximation, which tends to create artificial oscillations. Snodgrass and Kitanidis (1998) used an analytical solution of the transport equation to evaluate first-order and zero-order *in situ* reaction rates in the absence of sorption and negligible background concentrations. Schroth et al. (2001a) used the STOMP code (e.g., White and Oostrom, 2003) to simulate push–pull tests. STOMP is a well-tested finite-volume numerical code for one-, two- and three-dimensional simulations. To simulate conditions of linear non-equilibrium sorption, Schroth et al. (2001a) used the STAMMT-R code (Haggerty et al., 2000), which solves the multi-rate mass transfer equations for push–pull tests. A review of the literature on push–pull tests indicated that analysis of test data is often based on either analytical solutions with a number of simplifying assumptions or complex general-purpose codes that may not be easy to set up and run. The aim of this paper is to fill this gap.

This paper presents a one-dimensional, radial-coordinate, finite difference numerical model (PPTEST) that is well-suited for analyzing single-well push–pull test data, including commonly observed complexities, by eliminating the need for some of the simplifying assumptions inherent in the analytical solutions. The code is general enough to allow different sorption parameters and models, reaction orders, constants and lag times to be tested to describe a single dataset. In addition, microbial processes and Monod or Michelis–Menten kinetics can be simulated. It is expected that the improved estimates of parameters will provide better insights into the processes that control reactions initiated at mixing interfaces.

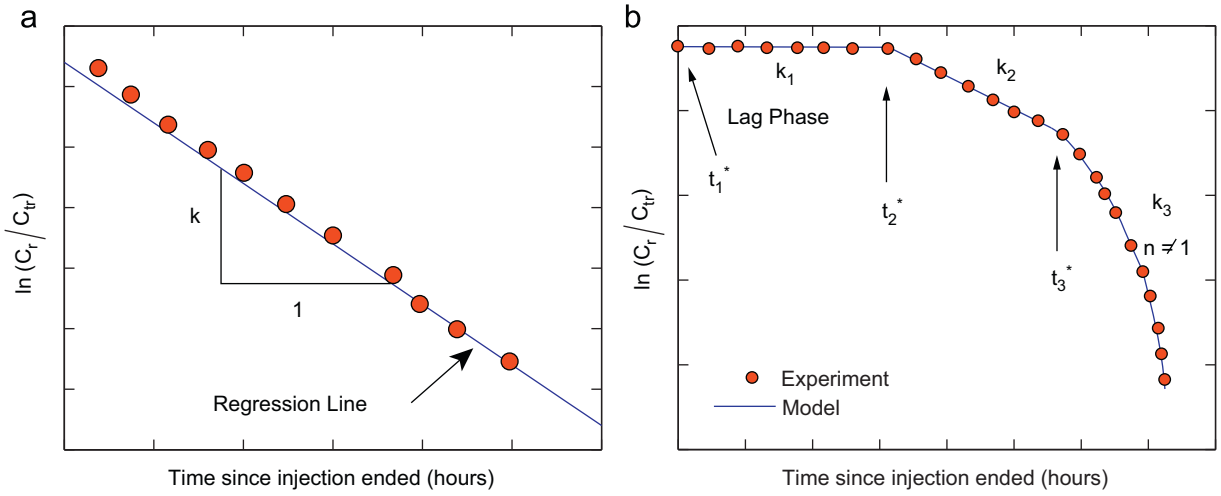

Fig. 2. (a) Example illustrating application of the simplified method of data analysis proposed by Haggerty et al. (1998). Here C_r and C_{tr} are concentrations of reactive component and tracer, normalized with respect to their injection concentrations, respectively. (b) Data obtained from some push–pull tests do not always plot as shown in Fig. 2(a). Multiple reaction rates, presence of a lag phase and potentially complex reaction order complicate rate interpretations.

2. Analysis

PPTEST is a radial coordinate model that solves equations for an arbitrary number of conservative and reactive constituents subjected to sorption and/or reactions in addition to advection and dispersion. The general governing equation for one-dimensional solute transport in radial coordinates in a homogeneous confined aquifer modified to account for multiple rate coefficients appears as shown below. Conservative solute transport follows as a special case of the more general equation presented below.

$$\frac{\partial C_i}{\partial t}+\frac{\rho_b}{\theta}\frac{\partial S_i}{\partial t}+\frac{A}{r}\frac{\partial C_i}{\partial r}=\alpha_L\left|\frac{A}{r}\right|\frac{\partial^2 C_i}{\partial r^2}-\sum_{j=1}^{N-1}[\mathcal{H}(t-t_j^*)-\mathcal{H}(t-t_{j+1}^*)]k_j C_i^{n_j}\pm F_i \tag{1}$$

Here C_i and S_i are the aqueous and sorbed-phase concentrations of the ith reactive component, respectively, t is the time, r the radial distance from the well, ρ_b the bulk density, θ the porosity, α_L the longitudinal dispersivity, $\mathcal{H}$ the Heaviside step function, k_j and n_j are the reaction constant(s) and order(s), respectively, t_j^* are the times at which there is a change in the reaction constants or orders (or both, see Fig. 2), N is the total number of reaction constants used to describe the data and F_i is a general user-defined source or sink term to describe reaction terms that depend on other species including microbial processes and Monod or Michelis–Menten kinetics. The pore water velocity near the well is given by

$$v=\frac{A}{r}=\frac{Q}{2\pi b\theta r} \tag{2}$$

where Q is the injection ($Q_{inj}>0$) or extraction rate ($Q_{ext}<0$), b the aquifer thickness and θ the aquifer porosity. Eq. (2) assumes that molecular diffusion is negligible and that the pore water velocity varies with radial distance but does not change with time. The regional groundwater velocity is assumed to have negligible effect compared to the effects of imposed pumping (a reasonable assumption close to the test well or for short time scales). Eq. (1) describes conservative solute transport when the sorption and reaction terms become zero. In PPTEST, the first species is always assumed to be a conservative solute although this behavior can be changed by invoking the user-defined reactions module which can be used to specify source and sink terms in all equations. Before solving Eq. (1), we need to invoke a sorption model. PPTEST allows simulations based on five different sorption models including three isotherm-based models, which include the Freundlich (Eq. 3), Langmuir (Eq. 4) and linear sorption (Eq. 5) models. In addition, one-site kinetic sorption (Eq. 6) and two-site sorption models (Eq. 7) are also included. The suffix i (which denotes the species number in Eq. (1)) is omitted in the following equations:

$$S=aC^{1/m} \tag{3}$$

$$S=\frac{pqC}{1+pC} \tag{4}$$

$$S=K_dC \tag{5}$$

$$\frac{\partial S}{\partial t}=\alpha(K_dC-S) \tag{6}$$

$$\frac{\partial S}{\partial t}=\alpha\left[(1-f)K_dC-S\right] \tag{7}$$

Details of the one- and two-site sorption models can be found in van Genuchten and Wagenet (1989). In the above equations, a, m, p, q are constants, α is a first-order kinetic sorption rate coefficient, K_d the distribution coefficient and f the fraction of exchange sites assumed to be in equilibrium in the two-site sorption model. The main difference between the Freundlich and Langmuir isotherms is that there is no capacity term (upper limit for sorption) in the Freundlich model while there is an upper limit in the Langmuir model (the parameter q denotes the capacity). For the isotherm-based models, if the S versus C relation is differentiated with respect to time and substituted into Eq. (1), then we obtain a single equation for the aqueous phase concentration with a retardation factor multiplying the unsteady term as shown below

$$R\frac{\partial C}{\partial t}+\frac{A}{r}\frac{\partial C}{\partial r}=\alpha_L\left|\frac{A}{r}\right|\frac{\partial^2 C}{\partial r^2}-\sum_{j=1}^{N-1}[\mathcal{H}(t-t_j^*)-\mathcal{H}(t-t_{j+1}^*)]k_j C^{n_j}\pm F \tag{8}$$

where the retardation factor is given by

$$R=1+\frac{\rho_b}{\theta}\frac{\partial S}{\partial C} \tag{9}$$

Substituting the S versus C relations in Eqs. (3–5) in Eq. (9), we get three different retardation factors for the three isotherm models (R_F, R_L or R) and a single equation (Eq. 8) is solved for the solute concentration C with one of the following retardation factors used (depending on the model selected by the user) in place of R in Eq. (8)

$$R_F=1+\frac{\rho_b m C^{m-1}}{\theta}$$

$$R_L=1+\frac{\rho_b}{\theta}\left(\frac{pq}{(1+pC)^2}\right)$$

$$R=1+\frac{\rho_b C}{\theta} \tag{10}$$

If the one-site or two-site sorption models are used then an additional Eq. (6) or (7) needs to be solved for the sorbed-phase concentration. In addition to the above sorption models, user-defined sorption models can be easily incorporated.

Eq. (1) differs from other similar equations in the push–pull test literature in two important ways. In addition to allowing multiple reaction constants and reaction orders, the reaction lag times t_i^* are important parameters that provide additional information about processes. Reactions can be modeled using one of two methods in PPTEST. In the first approach we use the second term on the right-hand side of Eq. (1). The summation sign and the Heaviside step function indicate that reactions with reaction lag time, arbitrary reaction order and multiple reaction constants can be used to describe data from a single push–pull test (Fig. 2b). Since the Heaviside unit step function operating on a function $f(x)$ has the following property:

$$[\mathcal{H}(t-t_j^*)-\mathcal{H}(t-t_{j+1}^*)]\,f(x)=\begin{cases}0 & \text{if } t<t_j^*\\ f(x) & \text{if } t_j^*<t<t_{j+1}^*\\ 0 & \text{if } t>t_{j+1}^*\end{cases} \tag{11}$$

the reaction term in Eq. (1) can be written for the ith species as

$$\sum_{j=1}^{N-1}[\mathcal{H}(t-t_j^*)-\mathcal{H}(t-t_{j+1}^*)]k_j C_i^{n_j}=\left\{\begin{matrix}k_1C_i^{n_1} & t_1^*\le t<t_2^*\\ 0 & otherwise\end{matrix}\right\}+\left\{\begin{matrix}k_2C_i^{n_2} & t_2^*\le t<t_3^*\\ 0 & otherwise\end{matrix}\right\}+\ldots+\left\{\begin{matrix}k_NC_i^{n_N} & t_{N-1}^*\le t<t_N^*\\ 0 & otherwise\end{matrix}\right\} \tag{12}$$

In the second approach, more complex reactions with source and sink terms as well as solute transport following the mobile–immobile approach can be modeled using the user-defined reaction module (which describes the term F_i for all equations similar to Eq. 1). Users can activate either one (or both) of the two reaction terms for different species.

2.1. Initial and boundary conditions

In what follows, we assume that Eq. (1) is coupled with either Eq. (6) or (7); hence, boundary and initial conditions are described for both aqueous and sorbed-phase concentrations. Prior to the start of the test, it is assumed that the background concentration for the test solution is zero. Alternatively, if the background concentrations are known, they can be specified as described in the PPTEST user manual. The initial conditions for solving Eqs. (1) and (6) or (7) are given by

$$C(r,t=0)=0 : r>r_w, \quad S(r,t=0)=0 : r>r_w \tag{13}$$

where r_w is the radius of the injection well. The boundary conditions used during injection and extraction phases are different, since both Q and v are positive during injection while they are negative during the extraction phase. The boundary conditions during the injection phase are a Robin condition near the well (for the aqueous phase) and a zero gradient condition at the outer edge of the boundary as shown below.

$$\begin{aligned}
&\left(-\alpha_L\frac{\partial C}{\partial r}+C\right)_{r=r_w}=C_0 : 0<t<t_{inj}\\
&S(r_w,t)=S_0 : 0<t<t_{inj}\\
&\frac{\partial C(r\to\infty,t)}{\partial r}=0\\
&\frac{\partial S(r\to\infty,t)}{\partial r}=0
\end{aligned} \tag{14}$$

During the injection phase some authors (Cassiani et al., 2005) used the following Dirichlet boundary condition near the well casing in place of the Robin condition shown in (11).

$$C_{r=r_w}=C_0 : 0<t<t_{inj} \tag{15}$$

Both types of boundary conditions were implemented in PPTEST although Eq. (15) is the default condition used (more details are available in the user manual). Boundary conditions for the injection of a chaser solution are similar in form to Eq. (14). After the injection period, a Robin boundary condition was used during the rest period since concentration changes only due to dispersion

$$\begin{aligned}
&\left(-\alpha_L\frac{\partial C}{\partial r}+C\right)_{r=r_w}=0 : t_{inj}<t<t_{rest}\\
&\frac{\partial S(r_w,t)}{\partial r}=0 : t_{inj}<t<t_{rest}\\
&\frac{\partial C(r\to\infty,t)}{\partial r}=0\\
&\frac{\partial S(r\to\infty,t)}{\partial r}=0
\end{aligned} \tag{16}$$

During the extraction phase Q and v are negative and a Neumann condition was used

$$\begin{aligned}
&\frac{\partial C(r_w,t)}{\partial r}=0 : t_{rest}<t<t_{ext}\\
&\frac{\partial S(r_w,t)}{\partial r}=0 : t_{rest}<t<t_{ext}
\end{aligned} \tag{17}$$

$$\begin{aligned}
&C(r\to\infty,t)\to 0 : t>0,\\
&S(r\to\infty,t)\to 0 : t>0
\end{aligned} \tag{18}$$

where t_{inj} is the injection time, t_{rest} the rest period between the injection and extraction phases and t_{ext} the extraction time. The pore water velocity is assumed to be zero during the rest period and C_0 is the initial concentration of the injected test solution.

2.2. Numerical model

An implicit, finite-difference numerical scheme was used for solving the governing equations. Important considerations in the development of the numerical model included mesh generation (e.g., to allow the placement of refined grids near arbitrary sampling well locations or near the well-casing) and advection schemes to accurately simulate situations with strong pumping. Several options are available to generate computational meshes for the 1D model. Variable step sizes following a geometric progression can be used to place fine grids near the well-casing. If this option is used, then the user specifies the desired spatial step size near the well (Δr_1) and the geometric ratio (λ). The program then computes the size of the computational domain (r_{max}) for a given number of points (n) using the formula

$$r_{max}=\frac{\Delta r_1(\lambda^n-1)}{(\lambda-1)} \tag{19}$$

The desired r_{max} value can be obtained by increasing or decreasing λ. In some push–pull tests it is not uncommon to have multi-level sampling wells placed at selected radial locations (Pickens et al., 1981). The ability to resolve details around sampling well locations is important for obtaining accurate numerical solutions. To generate computational meshes with refined spacing around an arbitrary radial location r_c, we used the following nonlinear transformation (Tannehill et al., 1997) that maps a vector of uniformly spaced grids r' (spanning between 0 and 1) to produce the desired clustering in r. Here γ is a tuning parameter that varies from zero (no stretching around r_c) to large values that produce most stretching around $r=r_c$.

$$\begin{aligned}
&B=\frac{1}{2\gamma}\ln\left[\frac{1+(e^{\gamma}-1)\left(\frac{r_c}{r_{max}}\right)}{1+(e^{-\gamma}-1)\left(\frac{r_c}{r_{max}}\right)}\right], \quad 0<\gamma<\infty\\
&r=r_c\left\{1+\frac{\sinh[\gamma(r'-B)]}{\sinh(\gamma B)}\right\}
\end{aligned} \tag{20}$$

Although previous numerical studies used second-order central differences to approximate the advection term (e.g., Hoopes and Harleman, 1967), we used a second-order accurate upwind scheme (Roache, 1998) to maintain numerical stability for advection-dominated situations. The program also provides the option to use a first-order accurate upwind difference scheme for the advection term. The dispersion term does not pose any numerical difficulty and was therefore approximated using central differences. The first and second derivatives were approximated using the following expressions for variable grids (Phanikumar and Mahajan, 1998):

$$\left.\frac{\partial C}{\partial r}\right|_j=\frac{C_{j+1}}{\beta_j(\Delta r_j+\Delta r_{j-1})}-\frac{\beta_j C_{j-1}}{(\Delta r_j+\Delta r_{j-1})}+\frac{(\Delta r_j-\Delta r_{j-1})}{(\Delta r_j\Delta r_{j-1})}C_j \tag{21}$$

$$\left.\frac{\partial^2 C}{\partial r^2}\right|_j=\frac{2}{(\Delta r_j+\Delta r_{j-1})}\left[\frac{C_{j+1}}{\Delta r_j}+\frac{C_{j-1}}{\Delta r_{j-1}}\right]-\frac{2C_j}{(\Delta r_j\Delta r_{j-1})} \tag{22}$$

$$\beta=\left(\frac{\Delta r_j}{\Delta r_{j-1}}\right) \tag{23}$$

where the index j denotes the node number, β is a mesh-expansion ratio and Δr_{j-1} and Δr_j are the step sizes to the left and right side of the node j, respectively. γ in Eq. (20) is a tuning parameter that controls the degree of grid clustering around $r=r_c$ and should not be confused with the mesh expansion ratio β defined in Eq. (23). Increase in γ will also increase β around $r=r_c$. Using the second-order upwind scheme, the advection term

in its conservative form was approximated as shown below (Roache, 1998).

$$\frac{\partial}{\partial r}(vC) = \frac{v_R C_R - v_L C_L}{\Delta}$$
$$v_R = \frac{1}{2}(v_{j+1} + v_j); \quad v_L = \frac{1}{2}(v_j + v_{j-1})$$
$$\left.\begin{array}{l} C_R = C_j \text{ if } v_R > 0 \\ C_R = C_{j+1} \text{ if } v_R < 0 \\ C_L = C_{j-1} \text{ if } v_L > 0 \\ C_L = C_j \text{ if } v_L < 0 \end{array}\right\} \quad (24)$$

where the subscripts R and L, respectively, refer to the right and left faces of the cell and Δ is an appropriate step size used to evaluate the first derivative depending on the direction of flow. The upwind difference scheme was implemented using four switches ψ_1,ψ_2,ψ_3 and ψ_4 whose integer values (+1, 0 or -1) change depending on the direction of the velocity (i.e., injection or extraction) as shown below

$$\frac{\partial}{\partial x}(vC) = \frac{v_R\psi_1 C_{j+1} + v_R\psi_2 C_j + v_L\psi_3 C_j + v_L\psi_4 C_{j-1}}{\Delta} \quad (25)$$

The implicit finite-difference representation of Eq. (1) appears as shown below

$$\frac{C_j^{\ell+1} - C_j^{\ell}}{\Delta t} + \frac{\rho_b}{\theta}\left(\frac{\partial S}{\partial t}\right)_j^{\ell} + \left(\frac{\psi_1 v_R C_{j+1}^{\ell+1} + \psi_2 v_R C_j^{\ell+1} + \psi_3 v_L C_j^{\ell+1} + \psi_4 v_L C_{j-1}^{\ell+1}}{\Delta}\right) = \alpha_L |v|_j^{\ell}\left\{\frac{2}{(\Delta r_j + \Delta r_{j-1})}\left[\frac{C_{j+1}^{\ell+1}}{\Delta r_j} - \frac{C_{j-1}^{\ell+1}}{\Delta r_{j-1}}\right] - \frac{2C_j^{\ell+1}}{(\Delta r_j \Delta r_{j-1})}\right\} - \sum_{i=1}^{N-1}[\mathcal{H}(t-t_i^*) - \mathcal{H}(t-t_{i+1}^*)]k_i (C_j^{\ell+1})^{n_i} + F_j \quad (26)$$

where $(\ell+1)$ and ℓ represent the new and old time-levels, respectively, and the suffix i is used as the index for the reaction constant and order ($i=1, \ldots, N$). Eq. (26) is written once for every grid node (j) and the resulting system of algebraic equations produces a tri-diagonal matrix, which can be solved efficiently using the Thomas algorithm (Press et al., 2007). Eq. (26) may be simplified by collecting terms

$$-\mathbf{E}_j C_{j-1}^{\ell+1} + \mathbf{F}_j C_j^{\ell+1} - \mathbf{G}_j C_{j+1}^{\ell+1} = \mathbf{R}_j \quad (27)$$

The right-hand side vector $\mathbf{R}_j$ in Eq. (27) is entirely made up of known concentration values at the previous time level, ℓ. However, if the kinetic or two-site sorption models are used, then two coupled equations (e.g., Eqs. (1) and (7)) need to be solved for the aqueous and sorbed-phase concentrations. For this case an additional system of equations similar to Eq. (26) is written for the S values and the vector $\mathbf{R}_j$ contains unknown sorbed-phase concentrations at the new time level $\ell+1$, which suggests an iterative procedure. The two systems of equations can be effectively decoupled since Eq. (7) can be used to explicitly solve for $S_j^{\ell+1}$ and then substituted into Eq. (26). The resulting decoupled system for $\mathbf{R}_j$ will only contain the aqueous phase concentrations at the previous time-level (Runkel and Chapra, 1993). To allow more complex sorption models in future versions, PPTEST solves the two equations (e.g., Eqs. (1) and (7)) separately by evaluating the unknown values at the previous time level as shown in Eq. (26) for the aqueous-phase concentration. This is justified due to the use of small temporal and spatial step sizes used in the numerical solution. The computational overhead for solving an additional 1D equation without spatial derivatives (such as Eq. (6) or (7)) is small. More details of the numerical scheme are available in the PPTEST user manual (Phanikumar, 2010). Coefficients of the tri-diagonal system (Eq. (27)) for the two-site sorption model appear as shown below

$$\frac{S_j^{\ell+1} - S_j^{\ell}}{\Delta t} = \alpha(1-f)K_d C_j^{\ell} - S_j^{\ell+1}$$
$$\mathbf{E}_j = 0$$
$$\mathbf{F}_j = \frac{1}{\Delta t} + 1$$
$$\mathbf{G}_j = 0$$
$$\mathbf{R}_j = \frac{S_j^{\ell}}{\Delta t} + \alpha(1-f)K_d C_j^{\ell} \quad (28)$$

Details of the Thomas algorithm are available in Press et al. (2007), Tannehill et al. (1997) and Roache (1998). Neumann and Robin boundary conditions were approximated to provide boundary values for the first and last grid nodes. The numerical scheme is stable and allows large time steps to be used.

3. Results and discussion

To evaluate the performance of PPTEST we compared results from the numerical model with approximate analytical solutions as well as field data obtained to estimate dispersion, sorption (Pickens et al., 1981) and reaction parameters (McGuire et al., 2002). Input files and sample output for all examples are available in the user manual (Phanikumar, 2010).

3.1. Comparison with analytical solution

Numerical solutions obtained using PPTEST were compared with the following approximate analytical solution developed by (Gelhar and Collins, 1971):

$$\frac{C}{C_0} = \frac{1}{2}\mathrm{erfc}\left[\frac{\left(\frac{V}{V_{inj}} - 1\right)}{\left\{\frac{16}{3}\left(\frac{\alpha_L}{r_{max}}\right)\left(2 - \left|1 - \frac{V}{V_{inj}}\right|^{1/2}\left(1 - \frac{V}{V_{inj}}\right)\right)\right\}^{1/2}}\right]$$
$$r_{\max} = \sqrt{\frac{Qt_{inj}}{\pi b \theta R}} \quad (29)$$

where V denotes the cumulative extracted volume ($=|Q_{ext}|t$), $V_{inj}=Q_{inj}t_{inj}$ and t_{inj} denotes the duration of the injection period. An upper limit for the applicability of Eq. (25) is $\varepsilon \ll 0.01$, where $\varepsilon=\alpha_L/2r_{max}$. Reasonable agreement was obtained between the numerical solution (obtained using a uniform grid of 1000 points) and the approximate analytical solution shown in Fig. 3 for $\varepsilon=0.0063$.

3.2. Comparison with field data (estimation of dispersion and sorption parameters)

Pickens et al. (1981) conducted push–pull tests in a sandy aquifer to understand the sorption of ^{85}Sr using ^{131}I as a conservative tracer. Tracer breakthrough curves (BTCs) were obtained at several radial distances ($r=0.36$, 0.66 and 2.06) and depths using multi-level sampling devices during the injection period. During the extraction period samples were collected from the well discharge line. The stratigraphic cross-section showed several horizontal layers and the tests were conducted in an 8 m thick layer, which is confined below by a 1 m silty clay unit and above by a 17 cm unit of silt and clay. Distribution coefficients for sorption (K_d) for ^{85}Sr obtained from breakthrough curves at three separate depths ranged from 2.6 to 4.5 mL/g. Mean porosity

and bulk density were calculated to be 0.38 and 1.7 g/cm^3, respectively. A total volume of 244 m^3 of test solution containing ^{131}I and ^{85}Sr was injected over a period of T_{inj}=94.32 h at a flow rate of Q_{inj}=2.587 m^3/h. There was no rest period and extraction pumping was done at the rate of Q_{ext}=2.282 m^3/h for 405.6 h. The data of Pickens et al. (1981) was also used by Schroth et al. (2001a) to test their approximate analytical approach. For our comparison we did not attempt to find the best-fit parameters that describe the data. Instead, PPTEST was used to simulate the data of Pickens et al. (1981) using the same parameters used by Schroth et al. (2001a). We used a variable mesh with finely spaced grids placed around r=0.36 m. This was accomplished using a tuning parameter β=10 in Eq. (16).The linear equilibrium sorption model (Eq. 6) was selected. Comparison of the observed and simulated ^{131}I and ^{85}Sr are shown in Fig. 4. All values of input parameters used for this comparison are given (and explained) in the PPTEST user manual. The non-reactive tracer was described well using α_L=6.4 cm and ^{85}Sr was described using linear equilibrium sorption with a retardation of R=11.4 (or K_d=2.33 mL/g). These results are in good agreement with the results of Schroth et al. (2001a).

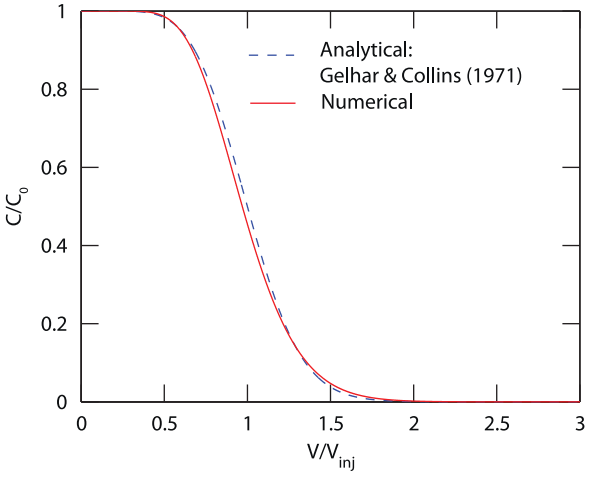

Fig. 3. Comparison of results obtained from PPTEST with an approximate analytical solution proposed by Gelhar and Collins (1971) for radial flow in an aquifer with advection and dispersion.

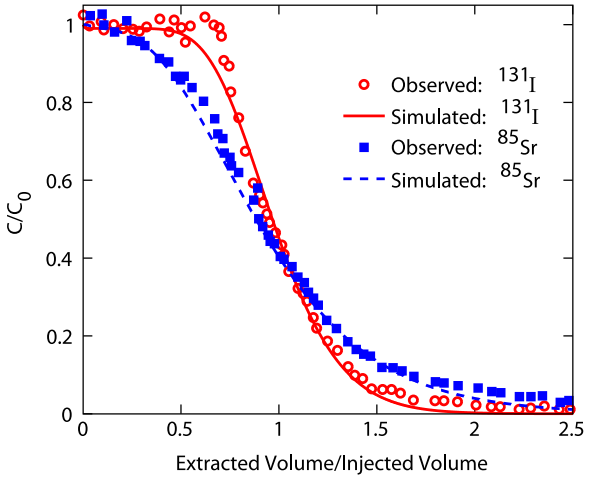

Fig. 4. Comparison of a numerical solution based on PPTEST with data of Pickens et al. (1981).

3.3. Comparison with field data (estimation of reaction rates)

McGuire et al. (2002) conducted a series of push–pull tests at the former Wurtsmith Air Force Base in Michigan. Their study was aimed at quantifying the rates of biogeochemical reactions when recharge water comes in contact with an anaerobic contaminated aquifer. The aquifer is composed of high-permeability aeolian and glacial outwash material. The tests were conducted in a well made of 2.5 cm inner diameter PVC casing. The injection and extraction rates were 0.0333 and 0.011 m^3/h, respectively. The injection period was followed by the injection of a chaser solution (deoxygenated, distilled deionized water) to flush the test solution from the well and to move it further into the aquifer. The durations of the injection, rest and extraction periods were 0.6, 0.0333 and 3.6 h, respectively. The chaser solution was injected for a period of 0.067 h. The concentrations of the tracer and the reactive solute are different during the two injection periods and this can be handled easily in PPTEST using a flag (ichasr) that determines whether or not a chaser solution was injected. The concentrations of chloride (tracer) and SO_4^{2-} during the injection period were 100 and 20 mg/L, respectively. All other input parameters are explained in the PPTEST user manual. Numerical solutions obtained using a uniform grid of 3001 points are shown in Figs. 5 and 6. Good agreement was obtained between the observed data and the numerical solutions. Sorption was not considered for SO_4^{2-} transport. A reaction lag period, two reaction constants (0.2 and 1.5 per hour) and times at which there is a change in slope ($t_1^* \approx 1.0$, $t_2^* \approx 2.6$) were important to describe the data. The need for two reaction constants can be clearly seen by the changes in the slope of the $\ln(C_r/C_{tr})$ versus time curve in Fig. 6(a). An alternative scenario in which a fractional-order reaction was used to describe the data is shown in Fig. 6(b). In this case, the observed data was described using a single reaction constant and order. Though there are several processes that might be the cause for these features, microbially mediated reactions can show fractional-order, for example, if there is a dependence on a substrate nearing depletion (e.g., (Madsen et al., 1999). PPTEST can be coupled with a parameter estimation routine such as PEST to automatically estimate these parameters.

3.4. User-defined reactions (comparison with analytical solutions)

To illustrate the application of the user-defined reactions module, we consider the following set of coupled differential equations with source terms. Eq. (31) has a degradation term that

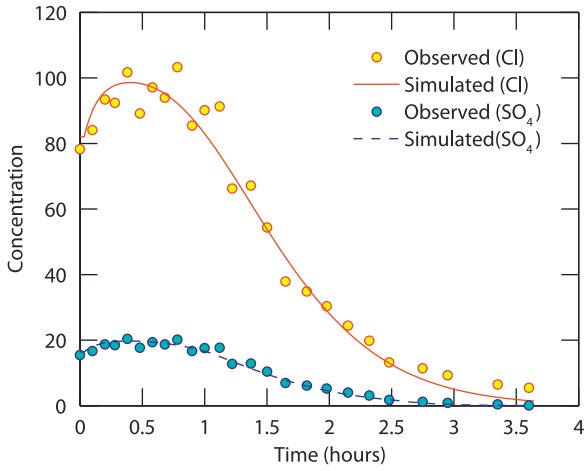

Fig. 5. Comparison of observed and simulated (PPTEST) concentrations of chloride and sulfate for an aquifer in Michigan (McGuire et al., 2002).

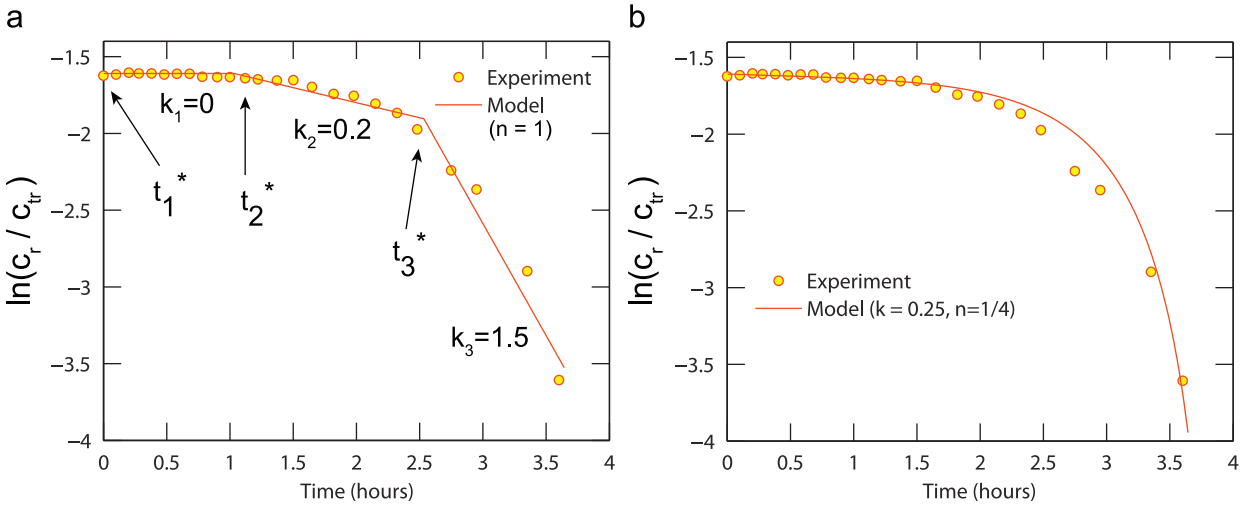

Fig. 6. Comparison of observed (McGuire et al., 2002) and simulated (PPTEST) concentrations of chloride and sulfate plotted as natural logarithm of relative concentrations of reactive component and tracer (chloride) versus time since injection. (a) Two reaction constants (0.2 and 1.5 per hour) were used to describe the data. (b) A fractional-order and a reaction constant of 0.25 were used to describe the data.

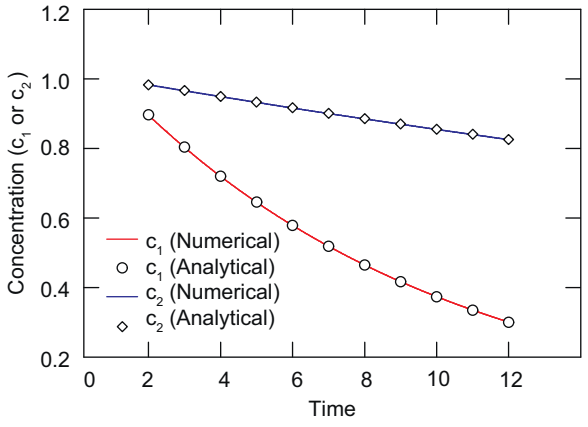

Fig. 7. Comparison of numerical (PPTEST) and analytical solutions for a coupled system of equations with source terms and Monod kinetics (k=0.2, k_S=0.1). Other parameters and details of the user-defined reactions module are available in the PPTEST user manual.

depends on the solution of Eq. (30) through the Monod term (k is a degradation rate and k_S denotes a half-saturation coefficient). The analytical solutions for this coupled system of equations were obtained using the method of manufactured solutions described in Roache (2009). Further details of the comparison are available in the PPTEST manual.

$$\frac{\partial C_1}{\partial t}+\frac{A}{r}\frac{\partial C_1}{\partial r}=\alpha_L\left|\frac{A}{r}\right|\frac{\partial^2 C_1}{\partial r^2}+S_1 \tag{30}$$

$$\frac{\partial C_2}{\partial t}+\frac{A}{r}\frac{\partial C_2}{\partial r}=\alpha_L\left|\frac{A}{r}\right|\frac{\partial^2 C_2}{\partial r^2}-k\left(\frac{C_1}{k_S+C_1}\right)C_2+S_2 \tag{31}$$

$$S_1=-\frac{1}{4r^{3/2}}e^{-\sqrt{r}t}\left(4r^2+2At+\alpha\left|\frac{A}{r}\right|t+\alpha\left|\frac{A}{r}\right|t^2\sqrt{r}\right) \tag{32}$$

$$S_2=-\frac{e^{-\frac{\sqrt{r}t}{2\pi}}}{16r^{3/2}\pi^2(k_S+e^{-\sqrt{r}t})}\left[\left(8r^2\pi+4At\pi+2\alpha\left|\frac{A}{r}\right|t\pi+\alpha\left|\frac{A}{r}\right|t^2\sqrt{r}\right)\times(k_S+e^{-\sqrt{r}t})-16ke^{-\sqrt{r}t}\pi^2r^{3/2}\right] \tag{33}$$

The system of equations has the following analytical solutions:

$$C_1=e^{-t\sqrt{r}},\quad C_2=e^{-t\sqrt{r}/2\pi} \tag{34}$$

Comparisons between the numerical and analytical solutions (Eq. 34) shown in Fig. 7 indicate that PPTEST has the ability to simulate coupled reactions using the user-defined reactions module.

4. Conclusions

In this paper we described the development of a numerical model that can be used to analyze push–pull test data in the presence of sorption, reaction lag times, multiple reaction constants and complex source/sink terms. Limitations of the model include the inability to handle regional gradients and heterogeneous formations. Comparisons with field data and analytical solutions showed that the numerical model has the ability to simulate a wide range of field conditions making it a useful tool for analyzing data and to test hypotheses related to various physical, chemical and biological processes.

Acknowledgements

This research was funded the National Science Foundation Biocomplexity in the Environment Grant #EAR-0418488/0935625.

Appendix A. Supplementary material

Supplementary data associated with this article can be found in the online version at doi:10.1016/j.cageo.2010.04.001.

References

Addy, K., Kellogg, D.Q., Gold, A.J., Groffman, P.M., Ferendo, G., Sawyer, C., 2002. In situ push–pull method to determine ground water denitrification in riparian zones. Journal of Environmental Quality 31, 1017–1024.

Cassiani, G., Burbery, L.F., Giustiniani, M., 2005. A note on in situ estimates of sorption using push–pull tests. Water Resources Research 41, W03005, doi:10.1029/2004wr003382.

Cunningham, J.A., Rahme, H., Hopkins, G.D., Lebron, C., Reinhard, M., 2001. Enhanced in situ bioremediation of BTEX-contaminated groundwater by

combined injection of nitrate and sulfate. Environmental Science and Technology 35, 1663–1670.
Davis, B.M., Istok, J.D., Semprini, L., 2002. Push–pull partitioning tracer tests using radon-222 to quantify non-aqueous phase liquid contamination. Journal of Contaminat Hydrology 58, 129–146.
Drever, J.I., McKee, C.R., 1980. The push–pull test a method of evaluating formation adsorption parameters for predicting the environmental effects on in-situ coal gasification and uranium recovery. In Situ 4, 181–206.
Gelhar, L.W., Collins, M.A., 1971. General analysis of longitudinal dispersion in nonuniform flow. Water Resources Research 7, 1511–1521.
Haggerty, R., Fleming, S.W., McKenna, S.A., 2000. STAMMT-R, Solute transport and multirate mass transfer in radial coordinates, Version 1.01, Technical Report SAND99-0164. Sandia National Laboratories, Albuquerque, New Mexico, 71pp.
Haggerty, R., Schroth, M.H., Istok, J.D., 1998. Simplified method of "push–pull" test data analysis for determining in situ reaction rate coefficients. Ground Water 36, 314–324.
Hall, S.H., Luttrell, S.P., Cronin, W.E., 1991. A method for estimating effective porosity and ground-water velocity. Ground Water 29, 171–174.
Harris, S.H., Istok, J.D., Suflita, J.M., 2005. Changes in organic matter biodegradability influencing sulfate reduction in an aquifer contaminated by landfill leachate. Microbial Ecology 51, 535–542.
Hoopes, J.A., Harleman, D.R.F., 1967. Dispersion in radial flow from a recharge well. Journal of Geophysical Research 72, 3595–3607.
Hsieh, P.A., 1986. A new formula for the analytical solution of the radial dispersion problem. Water Resources Research 22, 1597–1605.
Istok, J.D., Field, J.A., Schroth, M.H., 2001. In situ determinations of subsurface microbial enzyme kinetics. Ground Water 39, 348–355.
Istok, J.D., Field, J.A., Schroth, M.H., Sawyer, T.E., Humphrey, M.D., 1999. Laboratory and field investigation of surfactant-enhanced solubilization of trichloroethene. Ground Water 37, 589–598.
Istok, J.D., Humphrey, M.D., Schroth, M.H., Hyman, M.R., O'Reilly, K.T., 1997. Single-well "push–pull" test for in situ determination of microbial activities. Ground Water 35, 619–630.
Kleikemper, J., Schroth, M.H., Sigler, W.V., Schmucki, M., Bernasconi, S., Zeyer, J., 2002. Activity and diversity of sulfate-reducing bacteria in a petroleum hydrocarbon-contamianted aquifer. Applied and Environmental Microbiology 68, 1516–1523.
Kneeshaw, T.A., McGuire, J.T., Smith, E.W., Cozzarelli, I.M., 2007. Evaluation of sulfate reduction at experimentally induced mixing interfaces using small-scale push–pull tests in an aquifer-wetland system. Applied Geochemistry 22, 2618–2629.
Leap, D.I., Kaplan, P.G., 1988. A single-well tracing method for estimating regional advective veolcity in a confined aquifer: theory and preliminary laboratory verification. Water Resources Research 24, 993–998.
Luthy, L., Fritz, M., Bachofen, R., 2000. In situ determination of sulfide turnover rates in a meromitic alpine lake. Applied and Environmental Microbiology 66, 712–717.
Madsen, P.L., Thyme, J.B., Henriksen, K., Moldrup, P., Roslev, P., 1999. Kinetics of di-(2-ethylhexyl)phthalate mineralization in sludge-amended soil. Environmental Science & Technology 33, 2601–2606.
McGuire, J.T., Long, D.T., Klug, M.J., Haack, S.K., Hyndman, D.W., 2002. Evaluating the behavior of oxygen, nitrate, and sulfate during recharge and quantifying reduction rates in a contaminated aquifer. Environmental Science and Technology 36, 2693–2700.
Phanikumar, M.S., 2010. PPTEST: A multispecies reactive transport model to estimate biogeochemical rates based on single-well push-pull test data. Ver 2. user manual, Report, 2010ENE-01 Department of Civil & Environmental Engineering, Michigan State University, East Lansing, MI, 36pp. Available online: www.egr.msu.edu/~phani/pptest.
Phanikumar, M.S., Mahajan, R.L., 1998. Numerical analysis of unsteady thermo-solutal convection over a horizontal isothermal circular cylinder. Numerical Heat Transfer: Part A 33, 673–700.
Pickens, J.F., Grisak, G.E., 1981. Scale-dependent dispersion in a stratified granular aquifer. Water Resources Research 17, 1191–1211.
Pickens, J.F., Jackson, R.E., Inch, K.J., 1981. Measurement of distribution coefficients using a radial injection dual-tracer test. Water Resources Research 17, 529–544.
Pombo, S.A., Pelz, O., Schroth, M.H., Zeyer, J., 2002. Field scale 13C-labeling of phospholipid fatty acids (PFLA) and dissolved inorganic carbon: tracing acetate assimilation and mineralization in a petroleum hydrocarbon-contaminated aquifer. FEMS Microbiology Ecology 41, 259–267.
Press, W.H., Flannery, B.P., Teukolsky, S.A., Vetterling, W.T., 2007. Numerical Recipes: The Art of Scientific Computing 3rd ed. Cambridge University Press, Cambridge, UK 1256 pp.
Reinhard, M., Shang, S., Kitanidis, P.K., Orwin, E., Hopkins, G.D., Lebron, C.A., 1997. In situ BTEX biotransformation under enhanced nitrate and sulfate reducing conditions. Environmental Science and Technology 31, 28–36.
Roache, P.J., 1998. Fundamentals of Computational Fluid Dynamics, Revised edition. Hermosa Publishers, Alburqueue, NM 648pp.
Roache, P.J., 2009. Fundamentals of Verification and Validation. Hermosa Publishers, Albuquerque, NM 476pp.
Runkel, R.L., Chapra, S.C., 1993. An efficient numerical solution of the transient storage equations for solute transport in small streams. Water Resources Research 29, 211–215.
Schroth, M.H., Istok, J.D., Connoer, G.T., Hyman, M.R., Haggerty, R., O'Reilly, K.T., 1998. Spatial variability in in situ aerobic respiration and denitrification rates in a petroleum-contaminated aquifer. Ground Water 36, 924–937.
Schroth, M.H., Istok, J.D., Haggerty, R., 2001a. In situ evaluation of solute retardation using single-well push–pull tests. Advances in Water Resources 24, 105–117.
Schroth, M.H., Kleikemper, J., Bolliger, S.M., Bernasconi, S., Zeyer, J., 2001b. In situ assessment of microbial sulfate reduction in a petroleum-contaminated aquifer using push–pull tests and stable sulfur isotope analyses. Journal of Contaminat Hydrology 51, 179–195.
Senko, J.M., Istok, J.D., Suflita, J.M., Krumholz, L.R., 2002. In-situ evidence for uranium immobilization and remobilization. Environmental Science and Technology 36, 1491–1496.
Snodgrass, M.F., Kitanidis, P.K., 1998. A method to infer in situ reaction rates from push–pull experiments. Ground Water 36, 645–650.
Tannehill, J.C., Anderson, D.A., Pletcher, R.H., 1997. Computational Fluid Mechanics and Heat Transfer. Taylor & Francis, Washington, DC 896pp.
Ulrich, G.A., Breit, G., Cozzarelli, I.M., 2003. Sources of sulfate supporting anaerobic metabolism in a contaminated aquifer. Environmental Science and Technology 37, 1093–1099.
van Genuchten, M.T., Wagenet, R.J., 1989. Two-site/two-region models for pesticide transport and degradation: theoretical development and analytical solutions. Soil Science Society of America Journal 53, 1303–1310.
White, D.C., Oostrom, M., 2003. STOMP: Subsurface Transport over Multiple Phases. User's Guide. PNNL-14286. Pacific Northwest National Laboratory, Richland, WA 317pp.